Supplementary information

K⁺ extraction induced phase evolution of KFeO$_2$

Shiyu Zhang[a,b], Jian Sun[a,b], Jianghui Gao[a], Wen Jiang[a], Liwei Cheng[a,b], Hao Wang[a,b], Jun Lin[a,b], Cheng

Peng[a,b]*, Jianqiang Wang[a,b]*

[a] *Key Laboratory of Interfacial Physics and Technology, Shanghai Institute of Applied Physics, Chinese Academy of Sciences,*

Shanghai 201800, China

[b] *University of Chinese Academy of Sciences, No.19(A) Yuquan Road, Shijingshan District, Beijing 100049, China*

* Corresponding authors.

E-mail addresses: wangjianqiang@sinap.ac.cn (J. Wang), pengcheng@sinap.ac.cn (C. Peng).

Experimental Section

Materials. $KFeO_2$ was prepared via a conventional solid-state reaction method. Anhydrous K_2CO_3 (Sinopharm Chemical Reagent Co., Ltd., China) and Fe_2O_3 (Tianjin Bodi Co., Ltd., China) were mixed in stoichiometric ratio (1:1) and homogenized in agate mortar. The mixture (400 mg) was pressed into a sheet (with the diameter of 13 mm) and then placed in an alumina crucible for calcination in a tubular furnace (SK-G06123K-2, Tianjin Zhonghuan Experimental Furnace Co. Ltd., China). After sintering at 900 °C with a ramping rate of 5 °C min^{-1} for 5 h under argon atmosphere the stoichiometric $KFeO_2$ was obtained. The as-prepared $KFeO_2$ powder was exposed in ambient air (relatively humidity 75%, 25 °C) for 7 days and immersed in 500 mL Milli-Q water for 1 day, respectively, in order to investigate K^+ extraction. All of the samples were isolated in an argon-filled glove box to prevent ambient air.

Characterization. All samples were investigated by X-ray diffraction spectroscopy (XRD, Bruker AXS, D8 Advanced) using Cu Kα radiation source (λ=1.5418 Å) at 40 kV and 40 mA in range from 10° to 90°, with scanning rate 10° min^{-1} and step width 0.02°. The XRD patterns were Rietveld refined using TOPAS. The morphology and element distribution information were collected by a LEO 1530VP scanning electron microscopy (SEM, ZEISS) with an EDS detector, and a Tecnai G2 F20 S-Twin high-resolution transmission electron microscopy (HR-TEM, FEI). Raman spectroscopy (LabRAM HR Evolution, Horiba) was performed in range from 100 cm^{-1} to 1200 cm^{-1} excited by laser 633 nm. UV-Vis absorption spectroscopy was performed via UV2600, SHIMADZU. Mössbauer spectra were collected by constant acceleration transmission mode with 57Co/Rh source at room temperature. The velocity was corrected by a 25 mm Fe foil, the isomer shift was related to the center of Fe at room temperature, and all of the Mössbauer data were analyzed by MossWinn software.[1-2] Fe K-edge X-ray absorption spectroscopy (XAS) were collected at BL14W1 of Shanghai Synchrotron Radiation Facility (SSRF), and

XAS data were analyzed via a Demeter program that integrated with the ATHENA program and ARTEMIS program.[3-4]

Ab initio molecular dynamics (AIMD) simulation. Firstly, both cell parameters and all ionic positions in the initial $KFeO_2$ cubic cell were fully relaxed in the geometry optimization calculations by using the Broyden-Fletcher-Goldfarb-Shanno (BFGS) algorithm.[5-8] Secondly, the $KFeO_2$ surfaces (200) were modeled using a $1\times1\times1$ slab model containing 64 atoms, which was taken from the optimized structure with ~15 Å of vacuum along x-axis between the periodic images of the surface. Ultra-soft potentials with a scalar relativistic correction generated with Rappe-Rabe-Kaxiras-Joannopoulos method (RRKJUS) were used to describe the electron-ion interactions.[9] Pseudo potentials K.pbe-spn-rrkjus_psl.1.0.0.UPF, Fe.pbe-nd-rrkjus.UPF, O.pbe-rrkjus.UPF, and H.pbe-rrkjus.UPF were used for potassium, iron, oxygen, and hydrogen, respectively. The exchange and correlation functional was approximated using the semi-local gradient corrected form proposed by Perdew, Burke, and Ernzerhof (PBE).[10] The van der Waals forces were accounted for by the Grimme DFT-D3 approach.[11-12] Spin polarization calculations were used to ensure accurate results due to the magnetic nature of the Fe. For the electronic integration in reciprocal space, the Brillouin zone was sampled according to the Monkhorst-Pack scheme using $5\times3\times3$ and $1\times3\times3$ k-point grids for the bulk structure and its surfaces, respectively. For all calculations the energy cutoff for the wave functions and for the charge density were equal to 30 Ry and 300 Ry respectively, and the threshold for self-consistency used was 1×10^{-6} eV. AIMD simulations were run at 300 K with a 0.5 fs time step within the NVT ensemble. In order to study the effect of water molecules on the surface structure stability of $KFeO_2$, the AIMD simulation box containing a single layer 2D $KFeO_2$ surface, and 3 water molecules were calculated. For comparison reasons, the AIMD simulation box containing a single layer 2D $KFeO_2$ surface without water molecules were also calculated.

All calculations were carried out with the freely available, open-source Quantum Espresso (version 6.0) package.

Reference

1. Klencsár, Z.; Kuzmann, E.; Vértes, A. User-friendly software for Mössbauer spectrum analysis. J. Radioanal. Nucl. Chem. 1996, 210 (1), 105-118.

2. Xia, Y. Progress In Mossbauer Spectroscopy. Nucl. Sci. Tech. 1990, 1 (Z1), 24-31.

3. Ravel, B.; Newville, M. Athena, Artemis, Hephaestus: data analysis for X-ray absorption spectroscopy using IFEFFIT. J. Synchrotron Radiat. 2005, 12 (4), 537-541.

4. Rehr, J. J.; Kas, J. J.; Vila, F. D.; Prange, M. P.; Jorissen, K. Parameter-free calculations of X-ray spectra with FEFF9. Phys. Chem. Chem. Phys. 2010, 12 (21), 5503-5513.

5. Broyden, C. G. QUASI-NEWTON METHODS AND THEIR APPLICATION TO FUNCTION MINIMISATION. Math. Comput. 1967, 21 (99), 368-381.

6. Fletcher, R. A NEW APPROACH TO VARIABLE METRIC ALGORITHMS. Comput. J. 1970, 13 (3), 317-322.

7. Goldfarb, D. A FAMILY OF VARIABLE-METRIC METHODS DERIVED BY VARIATIONAL MEANS. Math. Comput. 1970, 24 (109), 23-26.

8. Shanno, D. F. CONDITIONING OF QUASI-NEWTON METHODS FOR FUNCTION MINIMIZATION. Math. Comput. 1970, 24 (111), 647-656.

9. Rappe, A. M.; Rabe, K. M.; Kaxiras, E.; Joannopoulos, J. D. Optimized Pseudopotentials. Phys.Rev.B 1990, 41 (2), 1227-1230.

10. Perdew, J. P.; Burke, K.; Ernzerhof, M. Generalized gradient approximation made simple. Phys. Rev. Lett. 1996, 77 (18), 3865-3868.

11. Grimme, S.; Antony, J.; Ehrlich, S.; Krieg, H. A consistent and accurate ab initio parametrization of density functional

dispersion correction (DFT-D) for the 94 elements H-Pu. J. Chem. Phys 2010, 132 (15), 154104.

12.   Grimme, S.; Ehrlich, S.; Goerigk, L. Effect of the Damping Function in Dispersion Corrected Density Functional Theory. J.
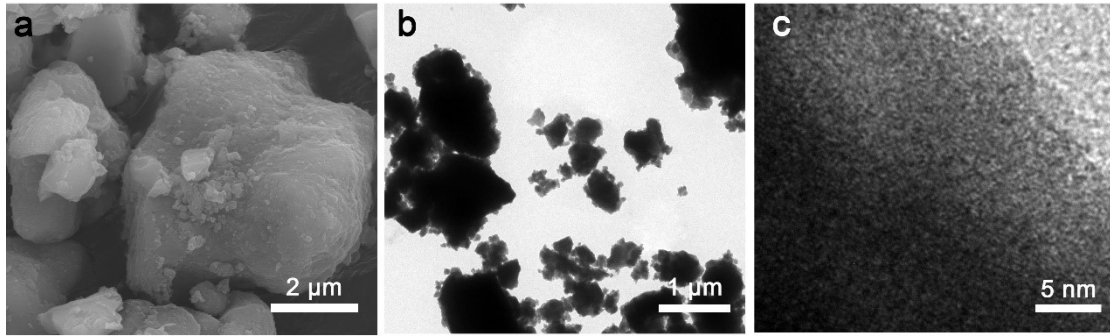
Comput. Chem 2011, 32 (7), 1456-1465.

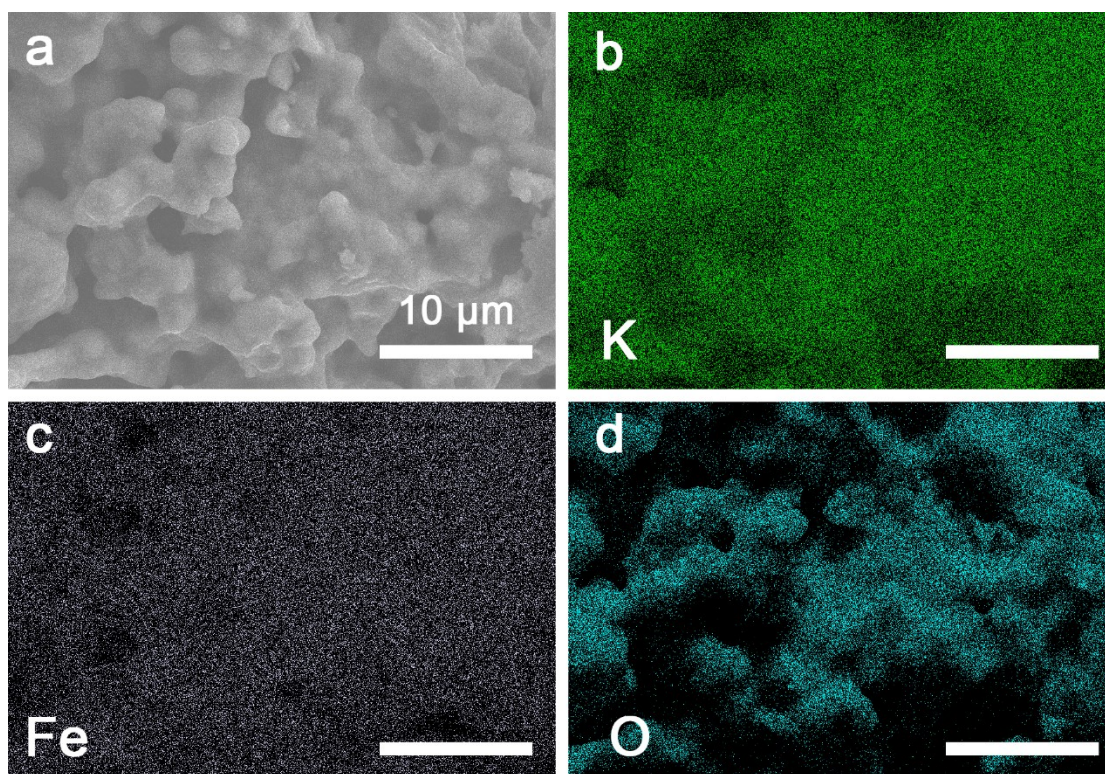**Figure S1.** The SEM (a) and HR-TEM (b, c) images of immersed KFeO$_2$.

Figure S2. The SEM image of fresh $KFeO_2$ and the EDS images of K (b), Fe (c) and O (d) distributions,
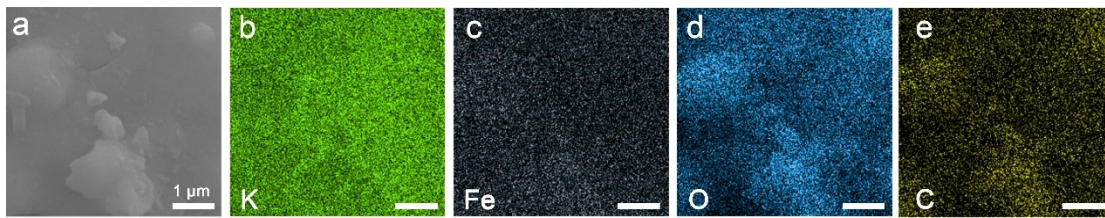
respectively.

Figure S3. The SEM image of exposed KFeO$_2$ (a) and the EDS images of K (b), Fe (c), O (d) and C (e) distributions, respectively.
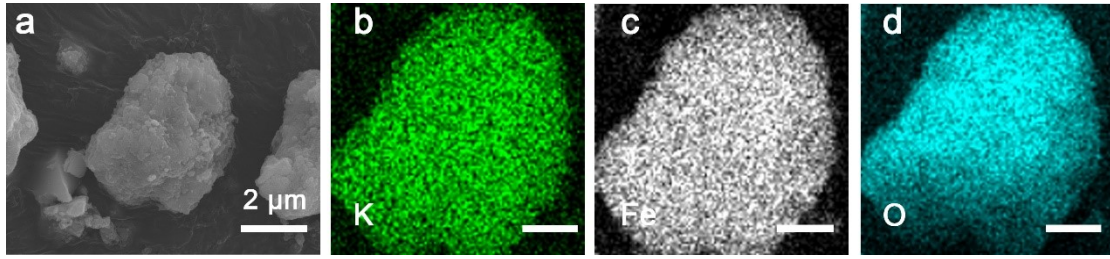
Figure S4. The SEM image of immersed KFeO$_2$ (a) and the EDS images of K (b), Fe (c) and O (d)
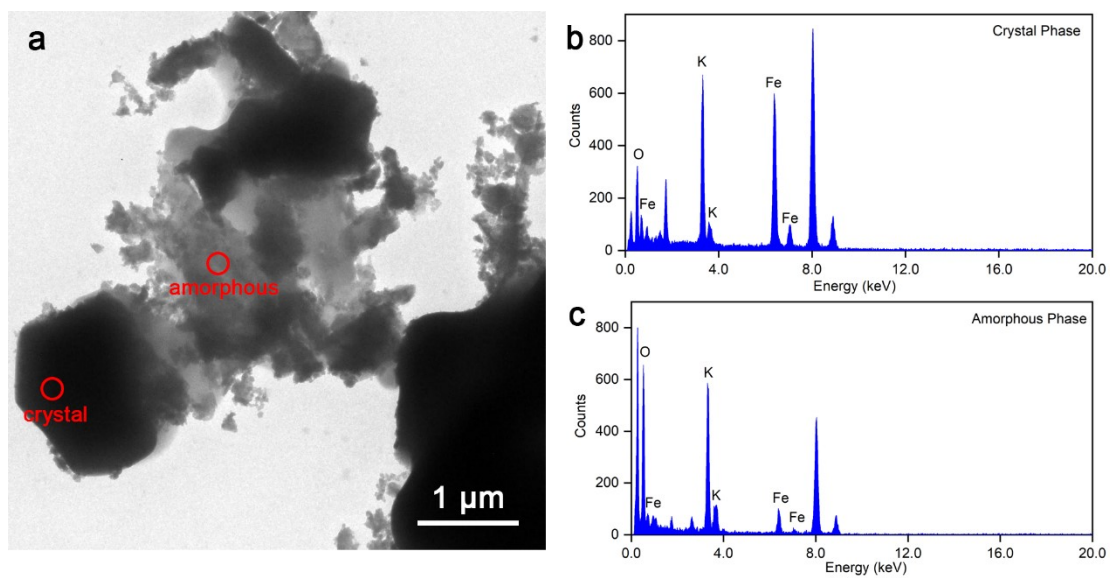
distributions, respectively.

Figure S5. The TEM image of exposed K_xFeO_2 (a), and the EDS spectra at the area of crystal phase (b) and amorphous phase (c), respectively.
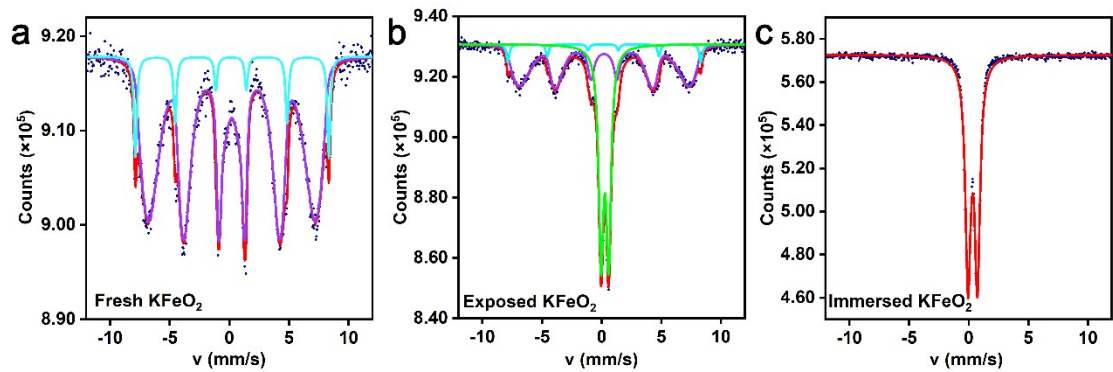
Figure S6. Mössbauer spectra of fresh (a), exposed (b) and immersed $KFeO_2$ (c) at room temperature.
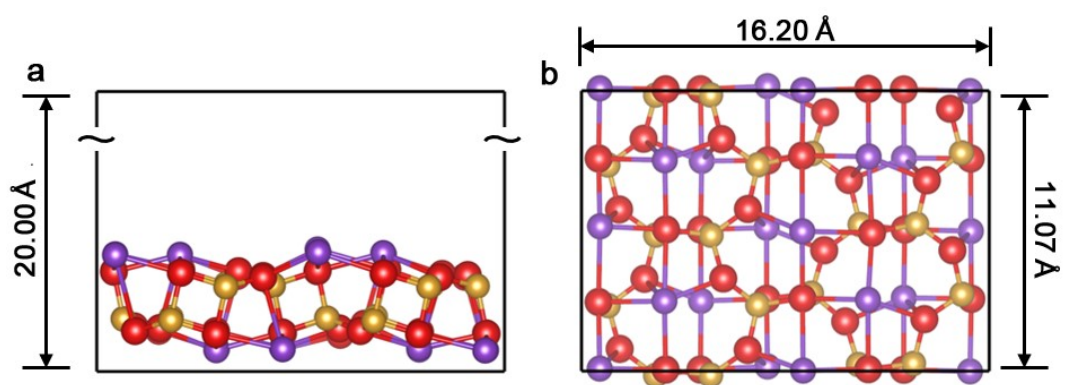
Figure S7. The side (a) and top (b) view of optimized (200) surface structure in KFeO$_2$.
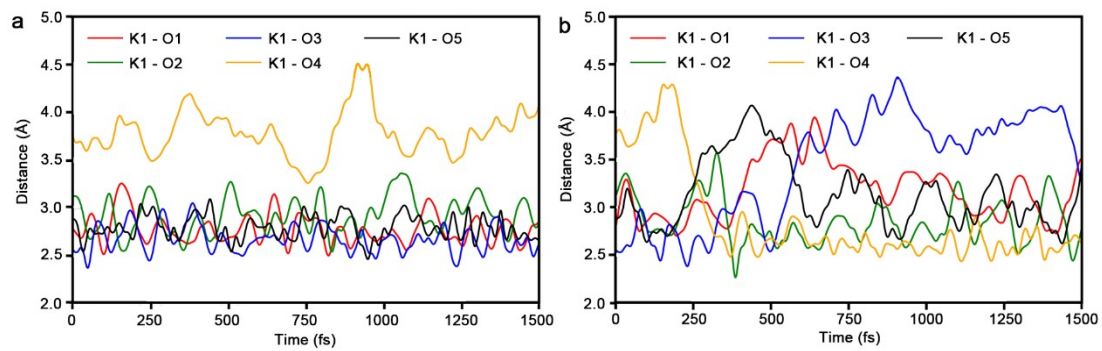
Figure S8 Time evolution of the distance between K1 and the adjacent five O atoms (O1, O2, O3, O4 and O5) in the absence (a) and presence of water molecules (b), respectively.
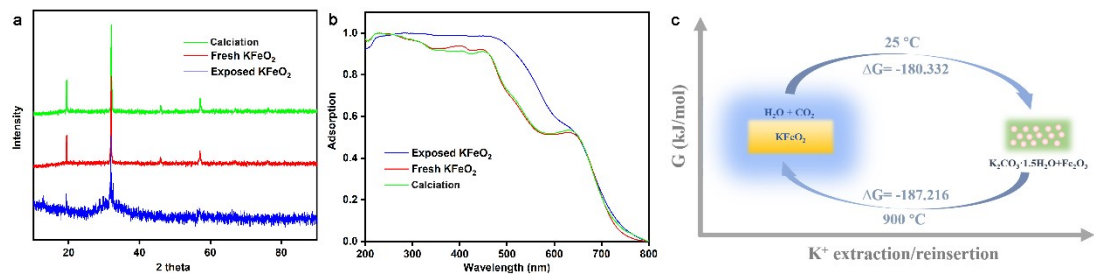
Figure S9. XRD (a) and UV-Vis absorption (b) spectra of fresh $KFeO_2$ and exposed $KFeO_2$ before and after calcination at 900 °C, and the illustration of Gibbs free energy changes of K^+-extraction at 25 °C and K^+-reinsertion at 900 °C (c), respectively.

Table S1. K, Fe, O and C contents (atom%) of fresh, exposed and immersed $KFeO_2$, respectively.

	fresh $KFeO_2$	exposed $KFeO_2$	immersed $KFeO_2$
K	25.03%	33.99%	9.85%
Fe	22.88%	16.24%	42.62%
O	52.08%	38.26%	47.54%
C	/	11.51%	/

Table S2. K, Fe and O contents (atom%) at the crystal and amorphous area on the surface of exposed

KFeO$_2$, respectively.

	crystal area	amorphous area
K	22.71%	21.15%
Fe	35.83%	3.65%
O	41.45%	75.18%

Table S3. Rietveld refinement parameters of the fresh and exposed $KFeO_2$, respectively.

		fresh $KFeO_2$	exposed $KFeO_2$
a/Å		5.580	5.596
b/Å		11.175	11.210
c/Å		15.747	15.772
V/Å³		981.987	989.37
	Fe1-O2	1.793	1.797
	Fe1-O3	1.879	1.885
Bond	Fe1-O4	1.984	1.989
Distance/Å	Fe2-O1	1.846	1.851
	Fe2-O2	1.866	1.871
	Fe2-O3	1.790	1.794
R_{wp}		3.53	2.76
GOF		1.20	1.16

Table S4. Mössbauer data of the fresh, exposed and immersed KFeO$_2$, respectively.

	IS (mm/s)	QS (mm/s)	LW	Mf (T)	Area (%)
fresh KFeO$_2$	0.209		0.358	37.935	89.27
	0.195	0.085	0.299	50.409	10.73
exposed KFeO$_2$	0.197		0.523	40.491	53.30
	0.180	0.095	0.293	50.292	4.53
	0.269	0.639	0.480		42.17
immersed KFeO$_2$	0.337	0.791	0.534		100

Table S5. Gibbs free energy values of $KFeO_2$ (s), H_2O (g), CO_2 (g), $K_2CO_3 \cdot 1.5H_2O$ (s) and Fe_2O_3 (s) at 25 °C and 900 °C, respectively.

G (kJ mol^{-1})	25 (° C)	900 (° C)	Ref
$KFeO_2$ (s)	-719.175	-884.958	1,2
H_2O (g)	-298.127	-489.478	2,3
CO_2 (g)	-457.240	-676.804	2,4
$K_2CO_3 \cdot 1.5H_2O$ (s)	-1674.056	-1972.898	5
Fe_2O_3 (s)	-849.059	-1020.829	2,4,5,6,7

K^+ extraction: $2KFeO_2(s) + 1.5H_2O(g) + CO_2(g) = K_2CO_3 \cdot 1.5H_2O(s) + Fe_2O_3(s)$ (ΔG= -180.334 kJ·mol^{-1}, 25 °C)

K^+ insertion: $K_2CO_3 \cdot 1.5H_2O(s) + Fe_2O_3(s) = 2KFeO_2(s) + 1.5H_2O(g) + CO_2(g)$ (ΔG= -187.216 kJ·mol^{-1}, 900 °C)

References:

1. Scientific Group Thermodata Europe, Grenoble Campus, 1001 Avenue Centrale, BP 66, F-38402 Saint Martin d'Héres, France, 1994.

2. Landolt-Börnstein: Thermodynamic Properties of Inorganic Material, Scientific Group Thermodata Europe (SGTE), Springer-Verlag, Berlin-Heidelberg, 1999.

3. JANAF Thermochemical Tables, 3rd ed., M.W. Chase, et. al.., eds., J. of Phys. and Chem. Ref. Data, Vol.14 , Suppl.1, pp. 1-1856, 1985.

4. Glushko Thermocenter of the Russian Academy of Sciences, IVTAN Association, Izhorskaya 13/19, 127412 Moscow, Russia, 1994.

5. Yungman V.S., Glushko V.P., Medvedev V.A., Gurvich L.V., Thermal Constants of Substances. Vol 1 - 8. New

York 1999.

6. Barin I: Thermochemical Data of Pure Substances, Part I, VCH Verlags Gesellschaft, Weinheim, 1993.

7. Barin I: Thermochemical Data of Pure Substances, Part II, VCH Verlags Gesellschaft, Weinheim, 1993.

Table S6. Rietveld refined fractional atomic coordinates, thermal factors (Beq), site occupancy factors

(SOF) of the fresh and exposed $KFeO_2$, respectively.

	Site	Wyckoff symbol	x	y	z	Beq	SOF
fresh $KFeO_2$	K1	8	0.769	0.004	0.074	2.00	1.00
	K2	8	0.811	0.260	0.185	2.00	1.00
	Fe1	8	0.249	0.008	0.184	2.00	1.10
	Fe2	8	0.280	0.261	0.064	2.00	1.10
	O1	8	0.583	0.291	0.022	4.00	1.20
	O2	8	0.166	0.410	0.099	4.00	1.20
	O3	8	0.287	0.171	0.158	4.00	1.20
	O4	8	0.089	0.481	0.282	4.00	1.20
exposed $KFeO_2$	K1	8	0.769	0.004	0.074	2.00	0.90
	K2	8	0.811	0.260	0.185	2.00	0.90
	Fe1	8	0.249	0.008	0.184	2.00	1.00
	Fe2	8	0.280	0.261	0.064	2.00	1.00
	O1	8	0.583	0.291	0.022	4.00	1.10
	O2	8	0.166	0.410	0.099	4.00	1.10
	O3	8	0.287	0.171	0.158	4.00	1.10
	O4	8	0.089	0.481	0.282	4.00	1.10